Check for updates

ADVANCED MATERIALS
www.advmat.de

Circularly Polarized Organic Ultralong Room-Temperature Phosphorescence with A High Dissymmetry Factor in Chiral Helical Superstructures

Jiao Liu, Zhen-Peng Song, Juan Wei, Jun-Jie Wu, Meng-Zhu Wang, Jian-Gang Li, Yun Ma, Bing-Xiang Li,* Yan-Qing Lu,* and Qiang Zhao**

Long-lived room-temperature phosphorescence (RTP) of organic materials holds a significant potential for optical information. Circularly polarized organic ultralong room-temperature phosphorescence (CP-OURTP) with extremely high dissymmetry factor (g_{lum}) values is even highly demanded and considerably challenging. Here, an effective strategy is introduced to realize CP-OURTP with an emission decay time of 735 ms and a g_{lum} value up to 1.49, which exceeds two orders of magnitude larger than previous records, through a system composed of RTP polymers and chiral helical superstructures. The system exhibits excellent stability under multiple cycles of photoirradiation and thermal treatment, and is further employed for information encryption based on optical multiplexing. The results are anticipated to lay the foundation for the development of CP-OURTP materials in advanced photonic applications.

1. Introduction

Persistent room-temperature phosphorescence (RTP) is an intriguing optical occurrence that endures for several seconds following the termination of the excitation source.[1,2] This attractive long-lasting afterglow phenomenon expands the dimension of luminescence signals, making them potentially valuable for applications in the fields of optical multiplexing, anti-counterfeiting, and information protection.[3–7] As a result, persistent RTP materials have attracted significant interest in recent years. Among various persistent RTP materials, organic ones represent a novel category that offers advantages such as facile preparation, flexibility, and cost-effectiveness compared to conventional inorganic counterparts, thus becoming a prominent research area.[8–13] To date, numerous organic persistent RTP materials have been extensively developed, and they have been successfully employed in various optical multiplexing applications, including sensing, imaging, and information encryption.[14–17] Current efforts concentrate on attaining superior and more advanced optical multiplexing applications. Consequently, an increase in the dimensions of optical signals is essential and challenging.

Integrating long-lived RTP with circularly polarized luminescence (CPL) serves as an effective approach to further expand the dimensionality of optical signals.[18–20] The quality of CPL can be characterized by the criterion:

$$g_{lum} = 2 \times \left(I_L - I_R\right) / \left(I_L + I_R\right) \quad (1)$$

where I_L and I_R represent the intensity of left-handed and right-handed CPL,[8] respectively. The highest g_{lum} of 2 represents completely left- or right-CPL.[9,10] Up to now, limited examples of organic luminescent materials featuring circularly polarized organic ultralong RTP (CP-OURTP) have been explored.[18–25] Ultralong phosphorescence refers to the luminescence phenomenon that is still maintained for a period of time (lifetime is >0.1 s) after the removal of the excitation source. These are often achieved through the aggregation of organic crystals,[20,21,23–26] which restrict the motion of chiral small molecules in polymeric skeletons[19,27] or confining in a rigid host matrix[18,22] (**Figure 1a**). To date, the g_{lum} values of reported long-lived RTP materials fall within the range of 10^{-3} to 10^{-2},[18–25] significantly lower than the theoretical maximum of 2.0. This is evidently not conducive to high-performance optical multiplexing. Consequently, it is highly

J. Liu, Z.-P. Song, J.-J. Wu, B.-X. Li, Q. Zhao
College of Electronic and Optical Engineering & College of Flexible Electronics (Future Technology)
Nanjing University of Posts and Telecommunications
Nanjing 210023, China
E-mail: bxli@njupt.edu.cn; iamqzhao@njupt.edu.cn

J. Wei, M.-Z. Wang, J.-G. Li, Y. Ma, Q. Zhao
State Key Laboratory for Organic Electronics and Information Displays & Jiangsu Key Laboratory for Biosensors
Institute of Advanced Materials (IAM)
Nanjing University of Posts and Telecommunications
Nanjing 210023, China
E-mail: iamyma@njupt.edu.cn

Y.-Q. Lu
National Laboratory of Solid State Microstructures & Collaborative Innovation Center of Advanced Microstructures & College of Engineering and Applied Sciences
Nanjing University
Nanjing 210093, China
E-mail: yqlu@nju.edu.cn

The ORCID identification number(s) for the author(s) of this article can be found under https://doi.org/10.1002/adma.202306834

DOI: 10.1002/adma.202306834

 © 2023 Wiley-VCH GmbH

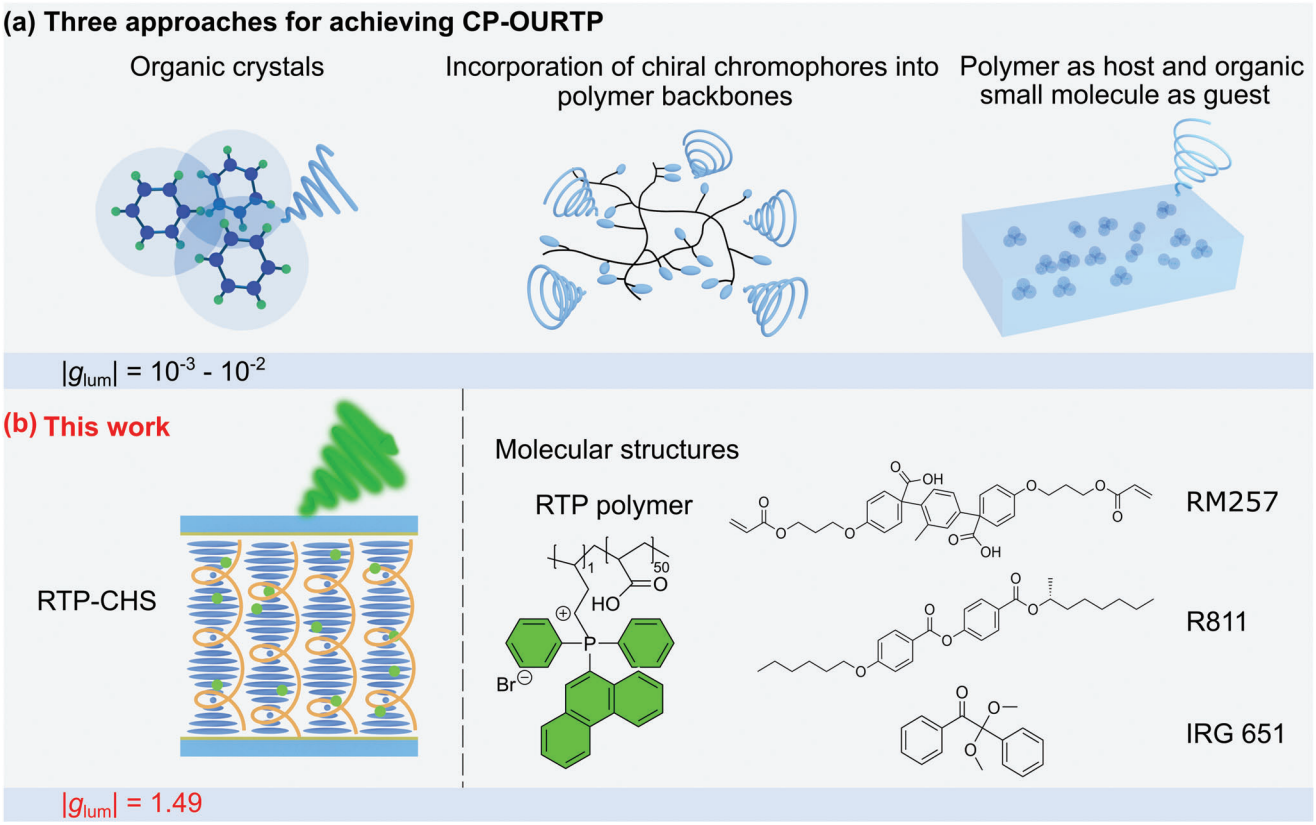

Figure 1. Three approaches for achieving circularly polarized organic ultralong room-temperature phosphorescence (CP-OURTP) and new strategy to boost the CP-OURTP in this work. a) Schematic illustration of organic materials demonstrating CP-OURTP performance by utilizing the strategies of organic crystals, incorporation of chiral chromophores into polymer backbones, and polymer as host and organic small molecule as guest. b) Schematic illustration of room-temperature phosphorescence (RTP) polymer-doped chiral helical superstructure (RTP-CHS).

desirable to develop a universal strategy for realizing persistent RTP with elevated g_{lum} values.

Previous studies have demonstrated that coupling luminophores with cholesteric liquid crystals (CLCs) is a potent strategy for achieving CPL with high g_{lum} values.[8,28,29] CLCs, serving as stimuli-responsive functional soft materials,[30–34] can selectively reflect circularly polarized light (i.e., photonic band gap, PBG) with the same handedness as helix due to their self-organized periodic helical superstructures.[35] As a result, CLCs are regarded as an ideal medium for enhancing chirality and generating CPL with ultra-high g_{lum} values. However, directly doping RTP molecules into liquid crystals (LCs) typically fails to produce long-lived phosphorescence emission since the loosely packed environment of LCs is unfavorable for stabilizing triplet excitons.[36,37] Alternatively, blending persistent RTP copolymers into LCs may effectively yield both long-lived RTP and high g_{lum} value of RTP, as multiple interactions among polymer chains can strictly restrict molecular motions of RTP molecules, resulting in inhibiting the non-radiative relaxation pathways.[22,23,38,39] Incorporating RTP copolymers into CLCs enables the integrity of the structural chirality of CLCs, which possess an intrinsic amplification effect, consequently, endowing CPL-active materials with a high g_{lum} value. Polymer-stabilized CLCs, which are chiral helical superstructure (CHS), provide a rigid mechanical environment to stabilize triplet excitons of RTP molecules, thus effectively reducing the non-radiative decay.[22]

In this work, we design and construct a long-lived RTP polymer-doped chiral helical superstructure (RTP-CHS) system. A distinct green afterglow can be observed upon the removal of 365 nm Ultraviolet (UV) excitation. More importantly, a g_{lum} value of persistent RTP was determined to be 1.49, which is over two orders of magnitude larger than previously reported g_{lum} values for organic phosphorescent materials (Figure 1b). Ultimately, optical multiplexing-based information encryption has been achieved, leveraging the remarkable features of simultaneously exhibiting long-lived RTP and an extremely high g_{lum} value.

2. Results and Discussions

2.1. Experimental Materials and Methods

Two organic materials but-3-en-1-yl(phenanthren-9-yl)diphenylphosphonium bromide and acrylic acid were selected for the preparation of the RTP polymer, because organic quaternary phosphonium derivative was reported to show intense persistent RTP in single molecular state and acrylic acid can provide rigid environment to stabilize triplet excitons. The RTP polymer was prepared by copolymerization in a molar ratio of 1:50, and the detailed synthetic procedures are illustrated in the Experimental Section. The monomer (M1) was characterized by ^{1}H nuclear magnetic resonance (NMR) spectroscopy, ^{13}C NMR spectroscopy, and

© 2023 Wiley-VCH GmbH

15214095, 2024, 7, Downloaded from https://advanced.onlinelibrary.wiley.com/doi/10.1002/adma.202306834 by Nanjing University, Wiley Online Library on [10/05/2025]. See the Terms and Conditions (https://onlinelibrary.wiley.com/terms-and-conditions) on Wiley Online Library for rules of use; OA articles are governed by the applicable Creative Commons License

high-resolution mass spectrometry (ESI-MS). The yield of the obtained copolymer was 93%, which was characterized by gel permeation chromatography (GPC), Power X-ray diffraction (PXRD) and ^{1}H NMR (Figures S1–S6, Supporting Information). The RTP-CHS films were fabricated as follows, taking a mixture of 60.3 wt.% HNG715600-100, 25.2 wt.% R811, 9.4 wt.% RM257, 0.1 wt.% Irgacure 651 of the photoinitiator, and 5 wt.% RTP polymer as an example. First, all constituents, excluding the RTP polymer, were mixed in dichloromethane (CH_2Cl_2) by vigorously stirring for 10 min to yield a homogeneous and transparent solution. The RTP polymer was dissolved in the mixture of CH_2Cl_2 and ethanol at 50°C, where the volume ratio of CH_2Cl_2 and ethanol is 1:1. Subsequently, these two prepared solutions were combined thoroughly, and the solvent was allowed to evaporate gradually at 70°C for 2 h. The obtained RTP-CHS mixture was spread on one glass substrate (Figure S7a,b, Supporting Information), which was coated with the 30 µm- diameter particles doped UV glue at four corners. Next, we covered another glass substrate on the first one and squeezed them slightly to obtain a uniform RTP-CHS film (Figure S7c, Supporting Information). Subsequently, the prepared LC cell underwent the polymerization process, which was irradiated with UV light (365 nm, ≈50 mw cm^{-2}, 1 min), and the afterglow emerged after the removal of UV light (Figure S7d,e, Supporting Information). A schematic illustration of the fabrication of RTP-CHS film was demonstrated in Figure S7 (Supporting Information). Further details can be found in the Experimental Section.

2.2. Photophysical Properties of RTP-CHS Films

The photophysical properties of the RTP polymer were studied by excitation spectrum (Ex), steady-state photoluminescence (PL), and delayed PL (Figure S8, Supporting Information). Afterward, the effect of relative humidity (RH) on RTP polymer was also investigated. When RH increases from 18% to 88%, the phosphorescence of RTP polymer is decreased by 64.0% in intensity (Figure S9a, Supporting Information) and 83.4% in lifetime (Figure S9b, Supporting Information). This issue that may limit practical applications could be resolved by using humidity controller or simply sealing RTP-CHS films in LC cells. To systematically investigate the photophysical properties of RTP-CHS, we prepared the RTP polymer as well as RTP-CHS films with various concentrations of the RTP polymer (C_{RTP} = 2, 5, and 10 wt.%). The absorbance spectrum of the CHS film (made of HNG715600-100, R811, RM257, and Irgacure 651) exhibits an intensive characteristic absorption band at 270–350 nm, which is assigned to be spin-allowed electronic transition (π-π*), and a lower energy absorption band was observed between 400–600 nm. Comparatively, the RTP polymer demonstrates an absorption band at 250–350 nm, which is attributed to intramolecular π-π, π-π* or n-π* transitions (Figure S10, Supporting Information). RTP-CHS films (C_{RTP} = 2, 5, and 10 wt.%) show the absorption peaks at 250–350 and 400–600 nm, primarily originating from the RTP polymer and CHS (Figure S10, Supporting Information). The reflectance spectra (upper) and PL emission band (bottom) of RTP-CHS films are characterized (Figure S11a, Supporting Information). The center wavelengths of the reflectance spectrums for different RTP-CHS films are located at the same wavelength of 520 nm, primarily arising from CHS. The PL spectra demonstrates two splitting peaks at emission wavelength (λ_{em}) of 490 nm and 520 nm upon irradiation of 300 nm UV light. We modulated the PBG of the CHS film to overlap with the emission peak of RTP polymer by selecting the concentration of R811 at 25.2 wt.%, which was regarded as a facile and efficient approach to achieve a high g_{lum} value. The effects of the concentration of LC polymer (C_{LCP}) on CPL signals, which consists of LC monomer (RM257) and the photoinitiator (Irgacure 651), were also studied carefully (Figure S11b, Supporting Information). As 2 wt.% < C_{LCP} < 5 wt.%, the g_{lum} values are 1.0 at 490 nm and 1.2 at 520 nm; when C_{LCP} increases from 5 wt.% to 10 wt.%, the g_{lum} can reach up to 1.49 at 490 nm and 1.25 at 520 nm; when C_{LCP} > 10 wt.%, no PBG in reflection of RTP-CHS can be observed in the wavelengths containing the emission band of RTP polymer, because the integrity of CHS will be significantly destroyed by LC polymer networks. Therefore, 10 wt.% LC polymer is regarded as the optimal concentration to attain a high g_{lum} value.

C_{RTP} is also a vital factor that affects the CPL signals, as shown in **Figure 2**a. RTP polymer, which is made of achiral molecules, shows no CPL signal. Meanwhile, the g_{lum} of CHS exhibits a relatively low value of 0.15 at ≈500 nm, which is likely due to the weak emission of CHS. It is evident that g_{lum} can reach the maximum of 1.49 at 490 nm, and 1.25 at 520 nm (C_{RTP} = 5 wt.%), then undergoes a decline to 0.52 at 490 nm and 0.48 at 520 nm (C_{RTP} = 10 wt.%). This result demonstrates that the CPL shows a pronounced increase behavior after encapsulating the RTP polymer into CHS (C_{RTP} < 5 wt.%). CPL signals of RTP materials are generally produced through aggregations of organic crystals, incorporation of chiral chromophores into polymer backbones, and polymer as host and organic small molecule as guest. However, in our system, we particularly selected CHS as matrix, because it possesses the periodic helical superstructure that can selectively reflect circularly polarized light with the same handedness and pass the opposite one due to PBG effect. The PBG of CHS was manipulated to overlap with the emission band of the RTP polymer by altering the concentration of R811, which is regarded as a valid approach to attain high g_{lum} values.[40–42] Overall, the CPL with high g_{lum} values could be largely boosted by introducing RTP polymer into CHS. Indeed, within the RTP-CHS system, a range of interactions, including ionic, ion-dipole, and dipole-dipole interactions, are believed to exist. These interactions contribute to the intricate architecture formed by the coexistence of the RTP polymer chains and CHS molecules. Therefore, the RTP polymer chains are physically dispersed inside the RTP polymer-CHS complex architectures and do not affect the LC structure of CHS, which is also demonstrated by the existence of PBG of RTP-CHS (Figure S11a, Supporting Information). Furthermore, we have conducted scanning electron microscopy (SEM) and energy-dispersive X-ray spectroscopy (EDS) mapping experiments on RTP-CHS films to confirm the uniform dispersion of RTP polymer (Figure S12, Supporting Information). Particularly, the EDS mapping image highlights the spatial distribution of phosphorous (P) elements, which are solely derived from the RTP polymer component (Figure S12c, Supporting Information). The uniform distribution of phosphorous elements throughout the CHS matrix, serves as compelling evidence for the homogeneous dispersion of the RTP polymer within the CHS matrix. This experimental evidence further substantiates the conceptual framework presented in the schematic illustration of Figure 1b. When C_{RTP} > 10 wt.%, photo-quenching occurs, giving rise to a decrease of g_{lum}. This behavior is similar to previously reported aggregation-induced emission dyes of HPS (1,1,2,3,4,5-Hexaphenylsilacyclopenta-2,4-diene) doped in bent-core LCs.[43] According to the above results, the specific RTP-CHS

© 2023 Wiley-VCH GmbH

15214095, 2024, 7, Downloaded from https://advanced.onlinelibrary.wiley.com/doi/10.1002/adma.202306834 by Nanjing University, Wiley Online Library on [10/05/2025]. See the Terms and Conditions (https://onlinelibrary.wiley.com/terms-and-conditions) on Wiley Online Library for rules of use; OA articles are governed by the applicable Creative Commons License

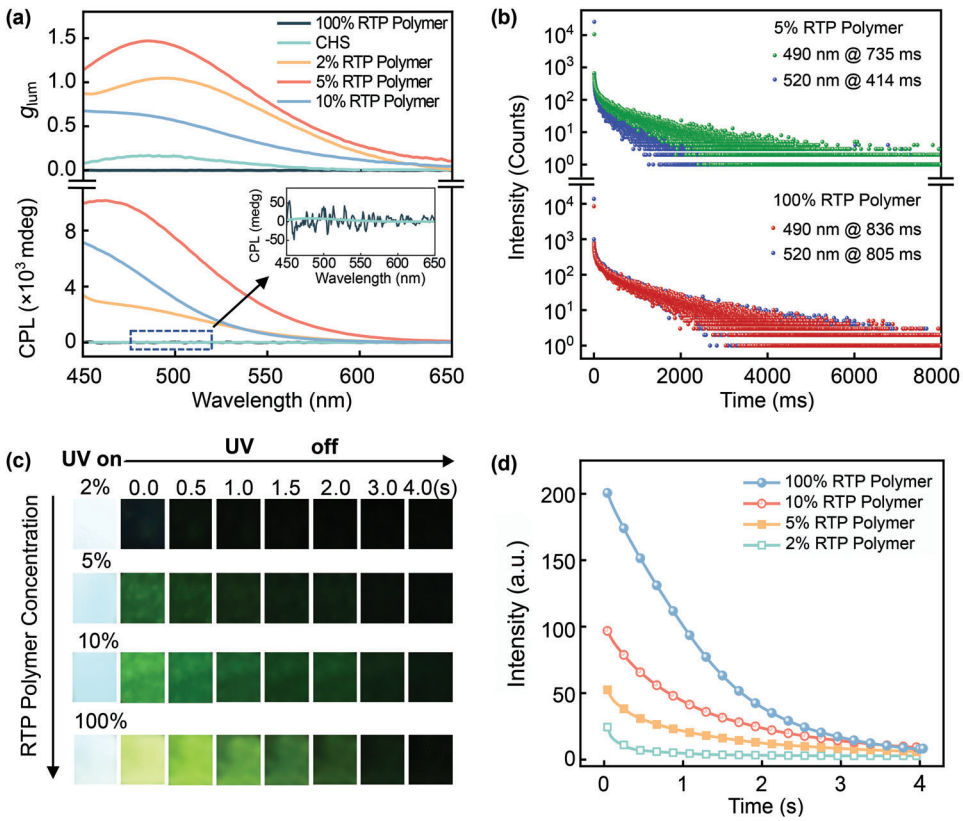

Figure 2. Photophysical properties of the RTP polymer and RTP-CHS. a) The g_{lum} value and CPL spectra of the RTP polymer, CHS, different concentrations of the RTP polymer in RTP-CHS films (C_{RTP} = 2, 5, and 10 wt.%, respectively). b) Lifetime decay profiles of 5 wt.% RTP-CHS (top), and pure RTP polymer (bottom) at the emission wavelength of 490 nm and 520 nm at 25°C. c) Photographs of RTP-CHS films (C_{RTP} = 2, 5, and 10 wt.%) and pure RTP polymer taken under irradiation of 365 nm UV light, and afterglow photographs captured by a Nikon camera at 25°C. d) Time-dependent afterglow intensity of the RTP polymer and different C_{RTP} in RTP-CHS films after the removal of UV light.

film (C_{RTP} = 5 wt.% and C_{LCP} = 10 wt.%) was prepared for further use.

As expected, the lifetimes of RTP polymer are longer (836 ms at λ_{em} = 490 nm and 805 ms at λ_{em} = 520 nm) compared with those of RTP-CHS films at C_{RTP} = 5 wt.% (735 ms at λ_{em} = 490 nm and 414 ms at λ_{em} = 520 nm). The reason is that the afterglow induced by the RTP polymer prefers rigid surroundings, whereas CHS films are somewhat fluidic, despite being treated by the polymerization process. The lifetimes of two other concentrations of RTP-CHS films (C_{RTP} = 2 wt.% and 10 wt.%) are also lower than those of pure RTP polymer and RTP-CHS film at C_{RTP} = 5 wt.% (Figures S13,S14, Supporting Information). The quantum yields of the RTP polymer and RTP-CHS films (C_{RTP} = 2, 5, and 10 wt.%) are 24.08%, 1.82%, 3.57%, and 7.10%, respectively (Figure S15, Supporting Information), which were determined using Edinburgh FLS 980 spectrometer with the integrating sphere of diameter 142 mm under ambient condition.

In addition, when excited by 365 nm UV light, RTP-CHS films (C_{RTP} = 2 wt.%, 5 wt.%, and 10 wt.%) and pure RTP polymer (C_{RTP} = 100 wt.%) all display an intense bright blue and homogeneous emission visible to naked eyes. Intriguingly, upon the removal of UV source, distinct green afterglows of RTP-CHS and pure RTP polymer were observed, gradually fading with a long luminescence lifetime of 4 s (Figure 2c). This phenomenon is likely ascribed to the rigid mechanical LC polymer networks, acting as polymer skeletons to stabilize the triplet excitons of RTP molecules. The pure RTP polymer, confined in a flower pattern, demonstrates a blue color upon irradiation of 365 nm UV, and a green color when the UV is turned off (Figure S16, Supporting Information). It is worth noting that the brightness of afterglow is consistent with the tendency of lifetime decay, that is, the afterglow intensity of pure RTP polymer is larger to the naked eyes, and the measured lifetimes are longer than those of different RTP-CHS films at C_{RTP} = 2, 5, and 10 wt.% (Figure 2b; Figures S13 and S14, Supporting Information). Figure 2d can give a more direct view on the changes of the time-dependent afterglow intensity as the decrease of C_{RTP} in RTP-CHS films after the removal of UV light, identifying the observations from Figure 2c.

2.3. Thermal Activities of Phosphorescent Afterglow

We further explored the temperature effect on the persistence of afterglow in RTP-CHS film. When an RTP-CHS film (C_{RTP} = 5 wt.%) was heated from 25 to 45°C, the intensity of afterglow gradually became brighter correspondingly, and then turned weak until it nearly vanished at 70 °C (**Figure 3**a). Additional evidence is supported by Figure 3b–d. These findings reveal that the

© 2023 Wiley-VCH GmbH

15214095, 2024, 7, Downloaded from https://advanced.onlinelibrary.wiley.com/doi/10.1002/adma.202306834 by Nanjing University, Wiley Online Library on [10/05/2025]. See the Terms and Conditions (https://onlinelibrary.wiley.com/terms-and-conditions) on Wiley Online Library for rules of use; OA articles are governed by the applicable Creative Commons License

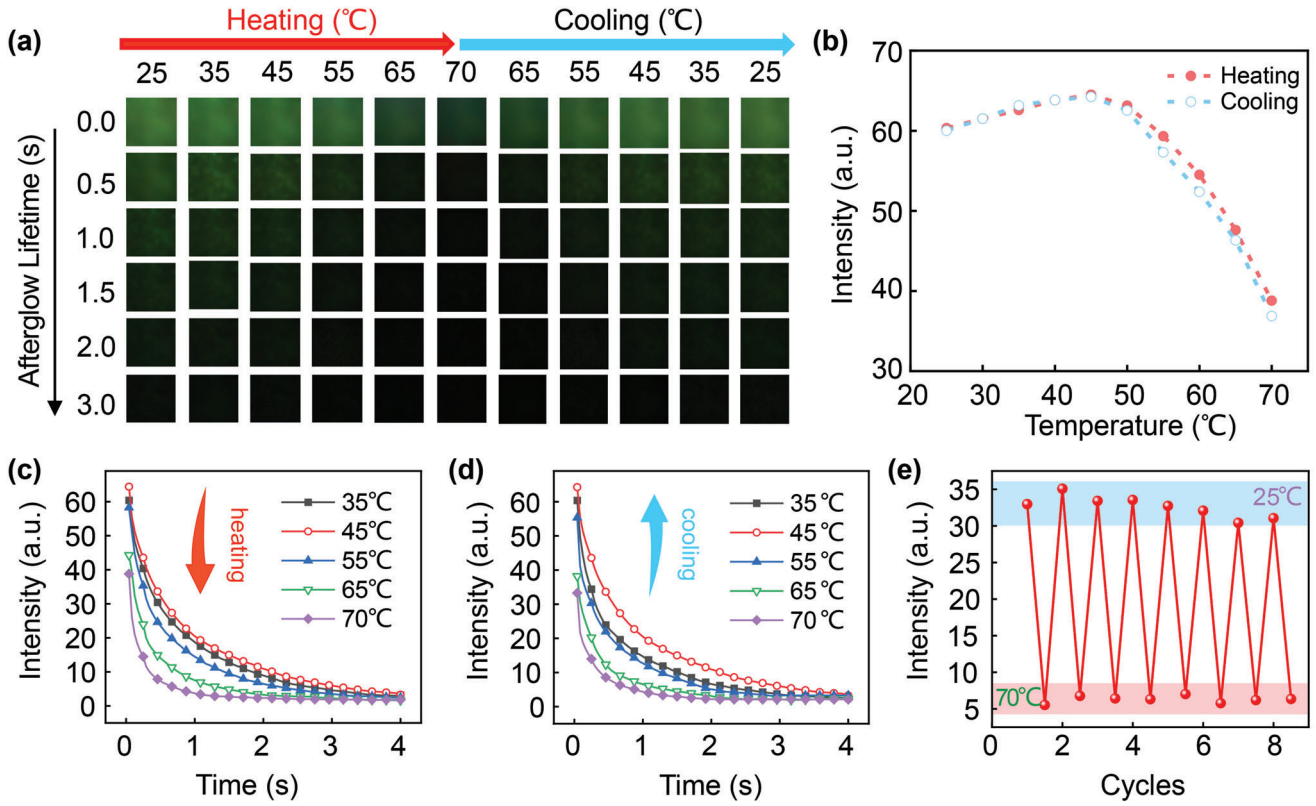

Figure 3. Afterglow reversible changes as the temperature varies in RTP-CHS system at C_{RTP} = 5 wt.%. a) Afterglow photographs taken under different temperatures captured by a Nikon camera. b) Temperature-dependent afterglow intensity (turning off UV in 0 s) during heating and cooling processes. c) Time-dependent afterglow intensity during the heating process from 35 to 70 °C after ceasing irradiation. d) Time-dependent afterglow intensity during the cooling process from 70 to 35 °C after ceasing irradiation of 365 nm UV. e) Reversible changes of afterglow intensity against repeated temperature cycles from 25 to 70 °C.

most favorable temperature for perceiving afterglow emission is 45 °C. RTP polymer, with its moisture absorption characteristic, immediately becomes viscous when taken out from the vacuum oven, which is desperately sensitive to the humidity. Elevating the temperature of RTP-CHS film to 45 °C effectively dissipated the moisture, leading to a gradual increase in the intensity of afterglow. However, high temperatures (> 50 °C) are capable of destructing the structure of rigid mechanical LC polymer networks since CHS is in its isotropic state, resulting in the decrease of afterglow intensity. Differential scanning calorimetry (DSC) measurement reveals that the phase transition of the RTP-CHS system (5 wt.%) occurs at −51.6 and 51.5 °C (Figure S17, Supporting Information). As shown in Figure S18 (Supporting Information), polarized optical microscopy photographs show typical oily streak textures,[44,45] thereby confirming that the phase identified by DSC in the temperature range from −51.6 to 51.5 °C represents the CHS LC phase. When the RTP-CHS film was cooled back to 25 °C, afterglow intensity experienced a reverted process with almost the same initial intensity (Figure 3e). These results suggest that the appropriate temperature and UV polymerization can significantly promote the stability of triplet excitons by the suppression of non-radiative transitions. Thus, the designed temperature-regulated device can be reversibly switched on and off under UV light. Additionally, we investigated the changes in afterglow intensity of pure RTP polymer with the variations of temperature (Figure S19, Supporting Information). For comparison, the thermal activities of pure RTP polymer were also explored (Figure S19a, Supporting Information). Unlike RTP-CHS film, the intensity of pure RTP polymer decreases all the time during the heating process from 25 to 70 °C; when cooling from 70 to 25 °C, the intensity can also revert back to the initial state (Figure S19b, Supporting Information).

2.4. Applications of RTP-CHS

The RTP-CHS films can be utilized for information encryption as shown in **Figure** 4a. When a left-handed circularly polarized filter (L-CPF) was placed on the top of the RTP-CHS photonic film under white light, the intensity of reflected light became weaker compared to that of the intensity without CPF. However, the RTP-CHS photonic film was clearly observed with a greenish color when a right-handed circularly polarized filter (R-CPF) was used. This result confirms that the obtained RTP-CHS photonic film possesses a right-handed helical structure, which can selectively reflect right-handed circularly polarized light, but transmit left-handed circularly polarized light. Additionally, under irradiation of 365 nm UV, the emissive RTP-CHS photonic film could

© 2023 Wiley-VCH GmbH

15214095, 2024, 7, Downloaded from https://advanced.onlinelibrary.wiley.com/doi/10.1002/adma.202306834 by Nanjing University, Wiley Online Library on [10/05/2025]. See the Terms and Conditions (https://onlinelibrary.wiley.com/terms-and-conditions) on Wiley Online Library for rules of use; OA articles are governed by the applicable Creative Commons License

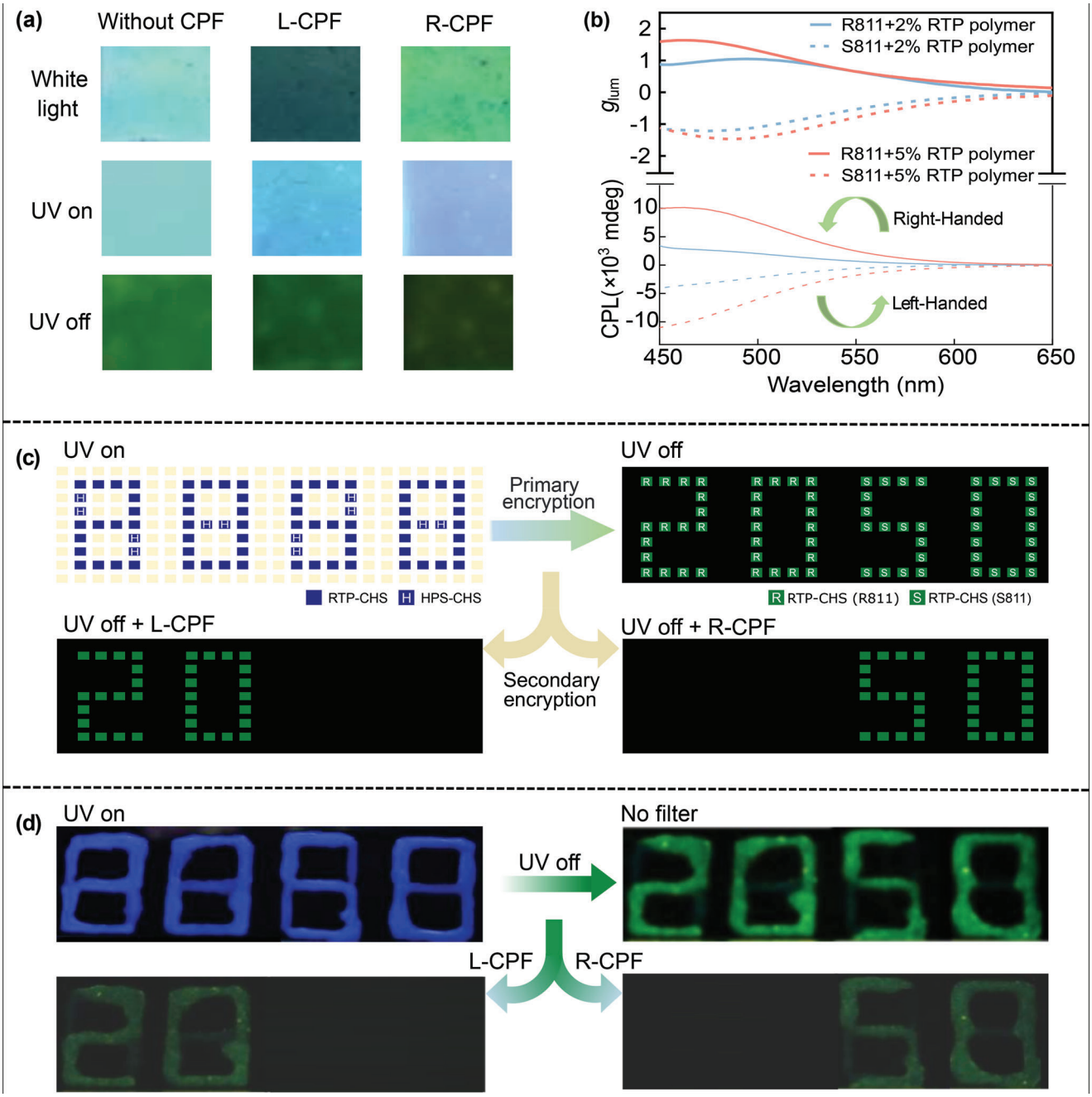

Figure 4. Applications of photoprogrammable RTP-CHS films. a) Photographs of RTP-CHS films taken without a circularly polarized filter (left, CPF), through a left-handed circularly polarized filter (middle, L-CPF) and a right-handed circularly polarized filter (right, R-CPF) under white light, under UV, and after the removal UV light. b) Mirror images of g_{lum} and CPL spectra of RTP-CHS films (C_{RTP} = 2 and 5 wt.%) with different chiral dopants of R811 and S811, respectively, depending on the wavelength (nm). c) Schematic illustration of optical multiplexing-based information encryption. d) Photographs of number patterns under the conditions of "UV on, UV off without filter, UV off with L-CPF, and UV off with R-CPF.

be identified by utilizing the L-CPF and R-CPF. Moreover, after the removal of 365 nm UV light, a homogeneous RTP-CHS photonic film with afterglow appeared with greenish color. The emissive film was more prominently perceived through L-CPF than R-CPF, suggesting that RTP-CHS photonic film can possess the distinct potential values in the application of the encryption field. Furthermore, we compared the chirality RTP-CHS films doped with chiral dopants of R811 and S811, respectively. The mirror images of CPL spectra (C_{RTP} = 2 wt.% and 5 wt.%) signify that the handedness of RTP-CHS photonic films can be well-controlled by chiral dopants (Figure 4b).

The optical multiplexing-based information encryption device was designed with a combination of distinct characteristics: long-lived RTP and high g_{lum} value RTP (Figure 4c). This was achieved

© 2023 Wiley-VCH GmbH

15214095, 2024, 7, Downloaded from https://advanced.onlinelibrary.wiley.com/doi/10.1002/adma.202306834 by Nanjing University, Wiley Online Library on [10/05/2025]. See the Terms and Conditions (https://onlinelibrary.wiley.com/terms-and-conditions) on Wiley Online Library for rules of use; OA articles are governed by the applicable Creative Commons License

by utilizing components such as HPS doped CHS films (abbreviated as HPS-CHS) at the concentration of 0.5 wt.% and RTP-CHS films with R811 and S811, respectively (Figure 4d). Under the irradiation of 365 nm UV light source, the device displays the numbers "8", "8", "8", and "8" in blue color due to the similar emission color under the continuous UV light of HPS-CHS and RTP-CHS films. When the UV source is deactivated, the numbers "2", "0", "5", and "0" in green color became visible, which were triggered by the persistent phosphorescence of the RTP polymer incorporated into CHS, thus forming the primary layer of information encryption. Furthermore, the numbers "2" and "0" were made of RTP-CHS with R811, exhibiting opposite handedness to the numbers "5" and "0" composed of RTP-CHS with S811, as demonstrated by Figure 4c. Apparently, when an L-CPF is introduced, the numbers "2" and "0" become discernible, albeit faintly green, matching along with the positive CPL signal in Figure 4b (solid line). As expected, employing an R-CPF leads to the exclusive recognition of the numbers "5" and "0", which is corresponding to the negative CPL signal in Figure 4b (dash line), thereby constructing the secondary encryption. Overall, this device showcases the potential use of photonic films, in combination with chiral dopants and CPF for information encryption.

3. Conclusion

In summary, for most reported phosphor materials, the g_{lum} values are relatively low in the order of magnitude from 10^{-2} to 10^{-3}. However, there is a growing demand for RTP materials with long-lasting afterglow and high g_{lum} values. In this study, we managed to achieve a high g_{lum} of 1.49 and afterglow with lifetime of 735 ms by constructing a long-lived RTP-CHS system based on self-assembled CHS. Furthermore, a temperature-force regulated chiroptical switch based on RTP polymer was realized with great stability. As a result, an RTP-featured optical multiplexing-based information encryption has been successfully constructed by feat of distinct characteristics of long-lived RTP and an extremely high g_{lum} value RTP. Our findings show great potential in information security, chiroptical devices, and optical detector fields.

4. Experimental Section

Materials: All commercially available starting reagents and solvents were used directly without further treatment. The nematic LC mixture (HNG715600-100) was purchased from Jiangsu Hecheng Display Technology Co. LTD. The chiral dopants (R811/S811), UV initiator 2,2-Dimethoxy-1,2-diphenylethan-1-one (Irgacure 651), and the polymerizable LC monomer (RM257) were all purchased from Nanjing Leyao Technology Co., LTD. Dichloromethane (CH_2Cl_2) was purchased from Macklin. HPS was purchased from Shanghai Jizhi Biochemical Technology Co., LTD. Liquid crystal cells were purchased from Kaiwei photoelectric technology in Zhuhai. Quartz substrates were purchased from Prism Optics.

Synthesis of But-3-en-1-yl(phenanthren-9-yl)diphenylphosphonium bromide (M1): The 1.6 M hexane solution of n-BuLi (14.5 mL, 23.3 mmol) was added dropwise to an agitating super dry tetrahydrofuran (THF, 40 mL) solution of 9-Bromophenanthrene (5 g, 19.45 mmol) at −78°C under an inert atmosphere of nitrogen. After stirring for 1 h, chlorodiphenylphosphine (5.1 g, 23.3 mmol) was added into the mixture. The reaction was stirred at 25 °C for 12 h. But-3-en-1-yl(phenanthren-9-yl)diphenvlphosphonium bromide was purified through column chromatography (petroleum ether), yield 78%. In nitrogen atmosphere, But-3-en-1-yl(phenanthren-9-yl)diphenvlphosphonium bromide (2 g, 5.5 mmol) was added into the mixture of 4-bromo-1-butene (1.5 g, 11.0 mmol) and DMF (20 mL). The reaction was stirred at 120 °C for 24 h. The compound was purified through column chromatography (methanol: dichloromethane = 50 :1), yield 87%. ^{1}H NMR (400 MHz, $CDCl_3$, δ): 7.90-7.68 (m, 11H), 7.52-7.40 (m, 2H), 7.08-6.83 (m, 2H), 5.98-5.67 (m, 1H), 5.42-5.02 (m, 2H), 3.73-3.39 (m, 2H), 3.05 (s, 6H), 2.34-2.24 (m, 1H).^{13}C NMR (100 MHz, DMSO-d_6, δ): 140.35, 136.26, 134.48, 133.81, 135.04, 132.85, 132.15, 130.96, 128.09, 125.49 124.25, 121.14, 118.93, 117.27, 112.95, 18.49. HRMS: m/z = 417.1751 [M − Br].

Synthesis of RTP Polymer: But-3-en-1-yl(phenanthren-9-yl)diphenylphosphonium bromide was copolymerized with acrylic acid at the molar ratio of 1/50 was used. The polymer was prepared by copolymerization of the But-3-en-1-yl(phenanthren-9-yl)diphenylphosphonium bromide (23.7 mg, 0.0597 mmol, 1 eq) and acrylic acid (212.2 mg, 2.9852 mmol, 50 eq) by a radical polymerization with 2,2′-azobis(2-methylpropionitrile) (4 mg) as radical initiator at 65 °C under an argon atmosphere in dimethylformamide for 12 h. The resulting mixture was added into methanol to precipitate polymeric materials. Precipitation was repeatedly washed with methanol to give purified polymers. The weight average molecular weight (Mw, 38 500), the number average molecular weight (Mn, 36 400) were summarized (Table S1, Supporting Information). The Ex, PL, delayed PL, and time-decay spectra of the RTP polymer were measured. In detail, RTP polymer powder was sandwiched between two quartz plates (1.5 cm × 1.5 cm) for the measurements of Ex, PL, and delayed PL, and another two quartz plates of different sizes (1 cm × 1 cm) for the time-decay spectra measurement.

Preparation of RTP-CHS Films: RM257 (9.6 mg), negative nematic LC HNG715600-100 (60.4 mg) as the reactive nematic LCs, and Irgacure 651(0.1 mg) as the photoinitiator, R811 or S811(25.6 mg) as the chiral dopant were dissolved in 5 mL DCM under the action of ultrasound for 10 min to obtain a homogeneous and transparent solution. Subsequently, RTP polymer (5 mg) was dissolved in the mixture of DCM and ethanol (1:1 volume ratio), and then sonicated for 30 min at the settled temperature of 50°C on a hot plate to form a uniform solution. These two prepared solutions were mixed together thoroughly in a small vial of 10 mL, and the solvent gradually evaporated at 70°C for 2 h to obtain RTP-CHS mixture (C_{RTP} = 5 wt.%). The temperature in the experiments was controlled by a hot stage (TS102XY) and a temperature controller (mK2000B). The glass substrates (1 cm × 1 cm) were cleaned with deionized water and ethanol thoroughly under the ultrasound treatment for 10 min, and then dried at 95 °C. Next, the obtained RTP-CHS mixture was sucked out by capillary action and precoated on glass substrate. The particle spacers (diameter: 30 μm) doped UV glue was deposited on each of four corners of the same glass substrate. After covering another glass substrate on the first one, two glass substrates were squeezed to provide a homogeneous RTP-CHS film. The

© 2023 Wiley-VCH GmbH

15214095, 2024, 7, Downloaded from https://advanced.onlinelibrary.wiley.com/doi/10.1002/adma.202306834 by Nanjing University, Wiley Online Library on [10/05/2025]. See the Terms and Conditions (https://onlinelibrary.wiley.com/terms-and-conditions) on Wiley Online Library for rules of use; OA articles are governed by the applicable Creative Commons License

prepared cell was irradiated with UV light source (365 nm, ≈50 mw cm^{-2}, 1 min) and the afterglow appeared after removing UV (Figure S7, Supporting Information). Thus, RTP-CHS film was prepared for reflective spectrums and future measurements of UV–vis, PL and CPL. Meanwhile, the RTP-CHS films with different concentrations (2 wt.% RTP polymer and 2 wt.% LC polymer, 2 wt.% RTP polymer, and 5 wt.% LC polymer, 5 wt.% RTP polymer and 2 wt.% LC polymer, 5 wt.% RTP polymer, and 5 wt.% LC polymer) were obtained in a similar way.

Preparation of RTP Polymer Film: First, RTP polymer (2 mg) was dissolved in deionized water (2 mL). Then the mixture was sonicated for 10 min at 25 °C until transparent solution was obtained. Subsequently, taking out 10 µL solution to deposit on a glass substrate, and the solution was allowed to evaporated gradually at 25 °C to produce a uniform RTP polymer film.

Statistical Analysis: Five independent experiments were performed for the same materials. The statistical analysis of results were further conducted to obtain the mean value and the standard deviation by using Mathematica software. The results were presented by using the mean value in this work. The ratio of the standard deviation to the mean value was smaller than 5%.

Supporting Information

Supporting Information is available from the Wiley Online Library or from the author.

Acknowledgements

J.L., Z.-P.S., J.W. contributed equally to this work. The work was supported by the National Key R&D Program of China (nos. 2022YFA1204404 and 2022YFA1405000), the Natural Science Foundation of Jiangsu Province, Major Project (no. BK20212004), Natural Science Research Start-up Foundation of Recruiting Talents of Nanjing University of Posts and Telecommunications (no. NY222053), and National Natural Science Foundation of China (62322508).

Conflict of Interest

The authors declare no conflict of interest.

Data Availability Statement

The data that support the findings of this study are available from the corresponding author upon reasonable request.

Keywords

chiral helical superstructures, circularly polarized phosphorescence, information encryption, luminescent dissymmetry factor, room-temperature phosphorescence

Received: July 12, 2023
Revised: August 25, 2023
Published online: December 6, 2023

[1] R. Kabe, N. Notsuka, K. Yoshida, C. Adachi, *Adv. Mater.* **2016**, *28*, 655.
[2] J. Wang, X. Gu, H. Ma, Q. Peng, X. Huang, X. Zheng, S. H. P. Sung, G. Shan, J. W. Y. Lam, Z. Shuai, B. Z. Tang, *Nat. Commun.* **2018**, *9*, 2963.
[3] K. Jiang, X. Gao, X. Feng, Y. Wang, Z. Li, H. Lin, *Angew. Chem., Int. Ed.* **2020**, *59*, 1263.
[4] K. Jiang, Y. Wang, X. Gao, C. Cai, H. Lin, *Angew. Chem., Int. Ed.* **2018**, *57*, 6216.
[5] Y. C. Liang, S. S. Gou, K. K. Liu, W. J. Wu, C. Z. Guo, S. Y. Lu, J. H. Zang, X. Y. Wu, Q. Lou, L. Dong, Y. F. Gao, C. X. Shan, *Nano Today* **2020**, *34*, 100900.
[6] P. Long, Y. Feng, C. Cao, Y. Li, J. Han, S. Li, C. Peng, Z. Li, W. Feng, *Adv. Funct. Mater.* **2018**, *28*, 1800791.
[7] Z. Wang, Y. Liu, S. Zhen, X. Li, W. Zhang, X. Sun, B. Xu, X. Wang, Z. Gao, X. Meng, *Adv. Sci.* **2020**, *7*, 1902688.
[8] J. Bao, R. Lan, C. Shen, R. Huang, Z. Wang, W. Hu, L. Zhang, H. Yang, *Adv. Opt. Mater.* **2021**, *10*, 2101910.
[9] L. Frédéric, A. Desmarchelier, L. Favereau, G. Pieters, *Adv. Funct. Mater.* **2021**, *31*, 2010281.
[10] J. Zhao, P. Xing, *ChemPhotoChem* **2021**, *6*, 202100124.
[11] H. Zheng, P. Cao, Y. Wang, X. Lu, P. Wu, *Angew. Chem., Int. Ed.* **2021**, *60*, 9500.
[12] X. Zhang, L. Du, W. Zhao, Z. Zhao, Y. Xiong, X. He, P. F. Gao, P. Alam, C. Wang, Z. Li, J. Leng, J. Liu, C. Zhou, J. W. Y. Lam, D. L. Phillips, G. Zhang, B. Z. Tang, *Nat. Commun.* **2019**, *10*, 5161.
[13] N. Feng, Z. Wang, D. Sun, P. Sun, X. Xin, X. Cheng, H. Li, *Adv. Opt. Mater.* **2022**, *10*, 2102319.
[14] Y. Zhang, S. Yu, B. Han, Y. Zhou, X. Zhang, X. Gao, *Matter* **2022**, *5*, 837.
[15] B. Yang, H. Ni, H. Wang, Y. Hu, K. Luo, W. Yu, *J. Phys. Chem. C* **2020**, *124*, 23879.
[16] S. Jiang, N. A. Kotov, *Adv. Mater.* **2022**, *35*, 2108431.
[17] Y. Dai, J. Chen, C. Zhao, L. Feng, X. Qu, *Angew. Chem., Int. Ed.* **2022**, *61*, e202211822.
[18] Z. Huang, Z. He, B. Ding, H. Tian, X. Ma, *Nat. Commun.* **2022**, *13*, 7841.
[19] L. Gu, W. Ye, X. Liang, A. Lv, H. Ma, M. Singh, W. Jia, Z. Shen, Y. Guo, Y. Gao, H. Chen, D. Wang, Y. Wu, J. Liu, H. Wang, Y. X. Zheng, Z. An, W. Huang, Y. Zhao, *J. Am. Chem. Soc.* **2021**, *143*, 18527.
[20] H. Li, J. Gu, Z. Wang, J. Wang, F. He, P. Li, Y. Tao, H. Li, G. Xie, W. Huang, C. Zheng, R. Chen, *Nat. Commun.* **2022**, *13*, 429.
[21] W. Chen, Z. Tian, Y. Li, Y. Jiang, M. Liu, P. Duan, *Chemistry* **2018**, *24*, 17444.
[22] W. Huang, C. Fu, Z. Liang, K. Zhou, Z. He, *Angew. Chem., Int. Ed.* **2022**, *61*, e202202977.
[23] H. Li, H. Li, W. Wang, Y. Tao, S. Wang, Q. Yang, Y. Jiang, C. Zheng, W. Huang, R. Chen, *Angew. Chem., Int. Ed.* **2020**, *59*, 4756.
[24] H. Liu, D. D. Ren, P. F. Gao, K. Zhang, Y. P. Wu, H. R. Fu, L. F. Ma, *Chem. Sci.* **2022**, *13*, 13922.
[25] B. Yue, X. Feng, C. Wang, M. Zhang, H. Lin, X. Jia, L. Zhu, *ACS Nano* **2022**, *16*, 16201.
[26] Y. Gong, L. Zhao, Q. Peng, D. Fan, W. Z. Yuan, Y. Zhang, B. Z. Tang, *Chem. Sci.* **2015**, *6*, 4438.
[27] D. W. Zhang, M. Li, C. F. Chen, *Angew. Chem., Int. Ed.* **2022**, *61*, e202213130.
[28] Y. He, S. Lin, J. Guo, Q. Li, *Aggregate* **2021**, *2*, e141.
[29] Z. Li, R. Lan, J. Bao, W. Hu, M. Wang, L. Zhang, H. Yang, *ACS Appl. Mater. Interfaces* **2022**, *14*, 8490.
[30] H. K. Bisoyi, Q. Li, *Chem. Rev.* **2022**, *122*, 4887.
[31] H. K. Bisoyi, Q. Li, *Acc. Chem. Res.* **2014**, *47*, 3184.
[32] W. H. C. Yuan, Z. Zheng, B. Liu, H. K. Bisoyi, Y. Li, D. Shen, Y. Lu, Q. Li, *Sci. Adv.* **2019**, *5*, eaax9501.
[33] L. Wang, A. M. Urbas, Q. Li, *Adv. Mater.* **2020**, *32*, 1801335.
[34] Z. G. Zheng, Y. Li, H. K. Bisoyi, L. Wang, T. J. Bunning, Q. Li, *Nature* **2016**, *531*, 352.

© 2023 Wiley-VCH GmbH

15214095, 2024, 7, Downloaded from https://advanced.onlinelibrary.wiley.com/doi/10.1002/adma.202306834 by Nanjing University, Wiley Online Library on [10/05/2025]. See the Terms and Conditions (https://onlinelibrary.wiley.com/terms-and-conditions) on Wiley Online Library for rules of use; OA articles are governed by the applicable Creative Commons License

[35] Y. He, S. Zhang, H. K. Bisoyi, J. Qiao, H. Chen, J. Gao, J. Guo, Q. Li, *Angew. Chem., Int. Ed.* **2021**, *60*, 27158.
[36] S. Tian, H. Ma, X. Wang, A. Lv, H. Shi, Y. Geng, J. Li, F. Liang, Z. M. Su, Z. An, W. Huang, *Angew. Chem., Int. Ed.* **2019**, *58*, 6645.
[37] Y. Su, S. Z. F. Phua, X. Z. Y. Li, D. Jana, G. Liu, W. Q. Lim, W. K. Ong, C. Yang, Y. Zhao, *Sci. Adv.* **2018**, *4*, eaas9732.
[38] X. Ma, C. Xu, J. Wang, H. Tian, *Angew. Chem., Int. Ed.* **2018**, *57*, 10854.
[39] L. Gu, H. Shi, L. Bian, M. Gu, K. Ling, X. Wang, H. Ma, S. Cai, W. Ning, L. Fu, H. Wang, S. Wang, Y. Gao, W. Yao, F. Huo, Y. Tao, Z. An, X. Liu, W. Huang, *Nat. Photonics* **2019**, *13*, 406.
[40] C. T. Wang, K. Chen, P. Xu, F. Yeung, H. S. Kwok, G. Li, *Adv. Funct. Mater.* **2019**, *29*, 1903155.
[41] X. Yang, M. Zhou, Y. Wang, P. Duan, *Adv. Mater.* **2020**, *32*, 2000820.
[42] J. Liu, Z. P. Song, L. Y. Sun, B. X. Li, Y. Q. Lu, Q. Li, *Respons. Mater.* **2023**, *1*, e20230005.
[43] J. Liu, Y. Molard, M. E. Prevot, T. Hegmann, *ACS Appl. Mater. Interfaces* **2022**, *14*, 29398.
[44] T. J. White, S. A. Cazzell, A. S. Freer, D. K. Yang, L. Sukhomlinova, L. Su, T. Kosa, B. Taheri, T. J. Bunning, *Adv. Mater.* **2011**, *23*, 1389.
[45] H. Wang, H. K. Bisoyi, M. E. McConney, A. M. Urbas, T. J. Bunning, Q. Li, *Adv. Mater.* **2019**, *31*, 1902958.

© 2023 Wiley-VCH GmbH

15214095, 2024, 7, Downloaded from https://advanced.onlinelibrary.wiley.com/doi/10.1002/adma.202306834 by Nanjing University, Wiley Online Library on [10/05/2025]. See the Terms and Conditions (https://onlinelibrary.wiley.com/terms-and-conditions) on Wiley Online Library for rules of use; OA articles are governed by the applicable Creative Commons License